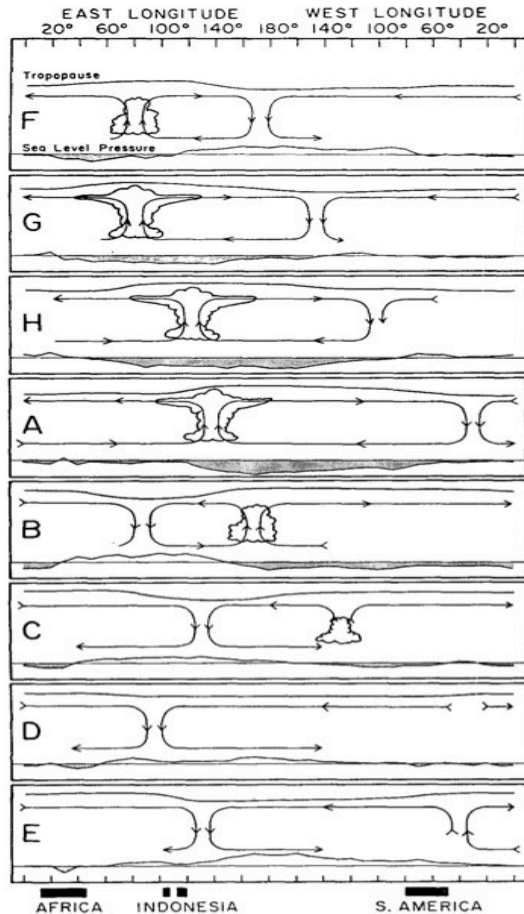


Amplified MJO impacts in California from eastward-extended teleconnection pattern

Wenyu Zhou (LBNL), Da Yang (UC Davis), Shang-Ping Xie (UCSD) and Jing Ma (NUIST)

Background and Motivation



Madden and Julian, 1972

□ Madden-Julian Oscillation (MJO)

- Dominating subseasonal mode in the tropics: planetary-scale and slow eastward propagation
- Excites Rossby-wave teleconnection that modulates extratropical weathers (e.g. atmospheric rivers, NAO)
- Important predictor for extended weather forecast beyond 2 weeks

□ How will the MJO extratropical teleconnection and impacts change under future warming?

Methods

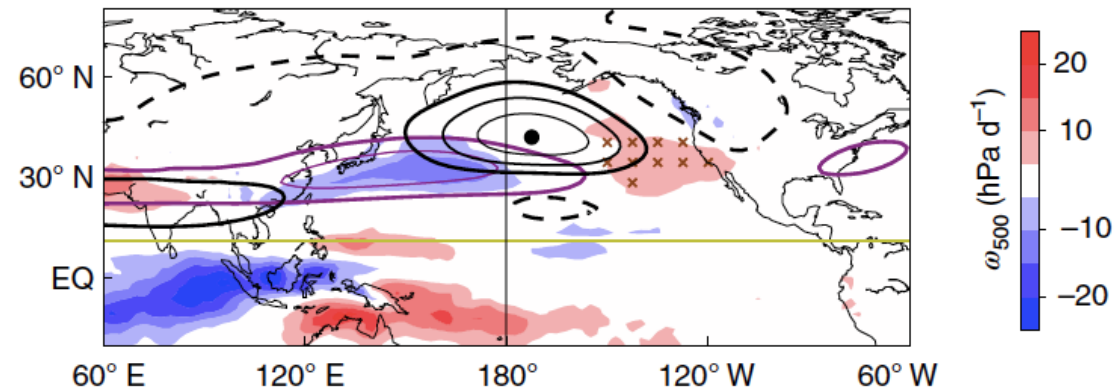
- ❑ Boreal winter (December-March) in the Northern Hemisphere
- ❑ Selected GCMs from CMIP5/6 (Precipitation East-West Power Ratio close to observations); HIST (1979-2005) and RCP8.5 (2079-2099)
- ❑ MJO-related diagnostics: MJO events and phase identified from real-time multivariable MJO indices (Wheeler & Hendon, 2014) and teleconnection pattern obtained as MJO-phase-composited fields

MJO teleconnection pattern extends eastward under future warming

Phase 3, HIST

PNA-like pattern anchored on the exit of the subtropical jet

Z_{250} (black contours), ω_{500} (shading), Precip (cross), \bar{U}_{250} (black contours)

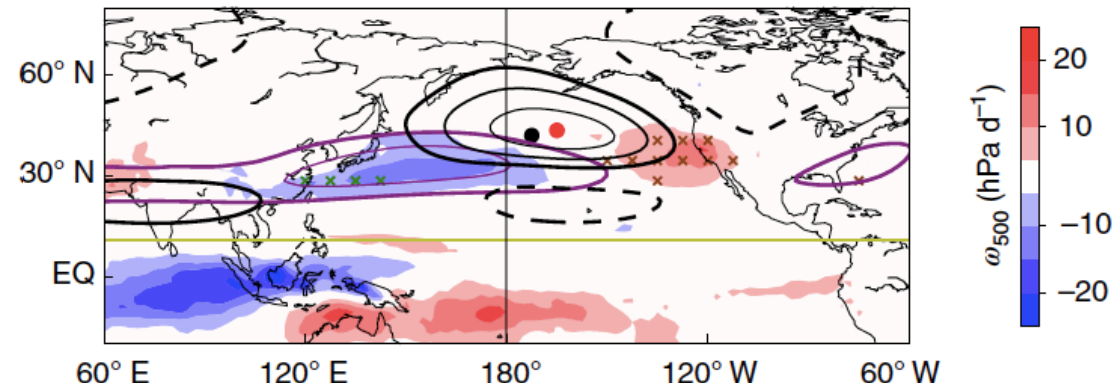


MJO teleconnection pattern extends eastward under future warming

Phase 3, RCP8.5

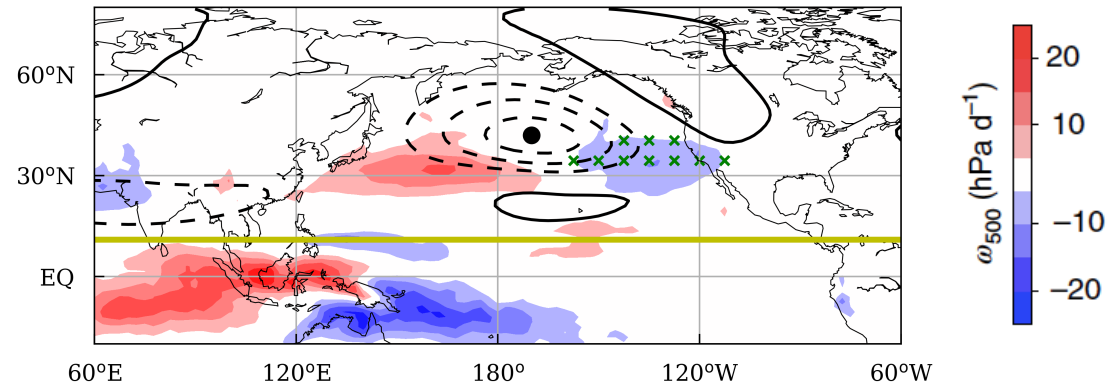
PNA-like pattern anchored on the exit of the subtropical jet

Z_{250} (black contours), ω_{500} (shading), Precip (cross), \bar{U}_{250} (black contours)



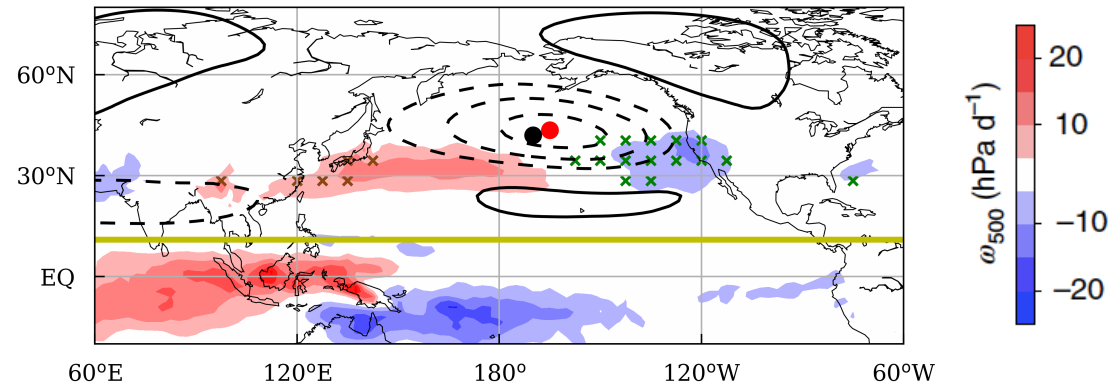
MJO teleconnection pattern extends eastward under future warming

Phase 7, HIST



MJO teleconnection pattern extends eastward under future warming

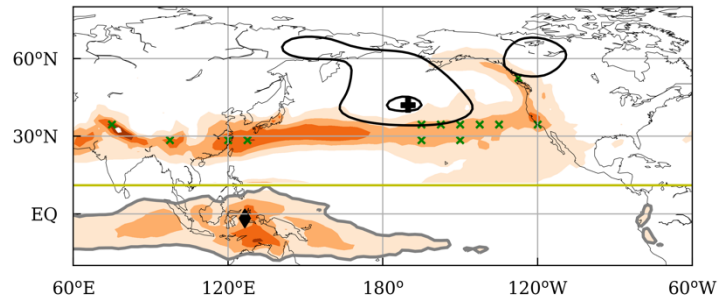
Phase 7, RCP8.5



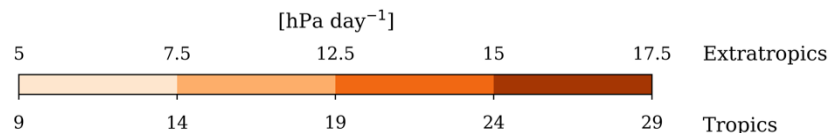
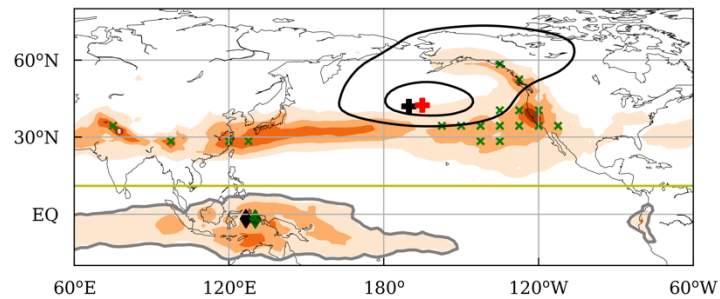
Amplified MJO impacts downstream in California

Variability throughout MJO phases
 Z_{250} (contours), ω_{500} (shading)
 and Precip (cross)

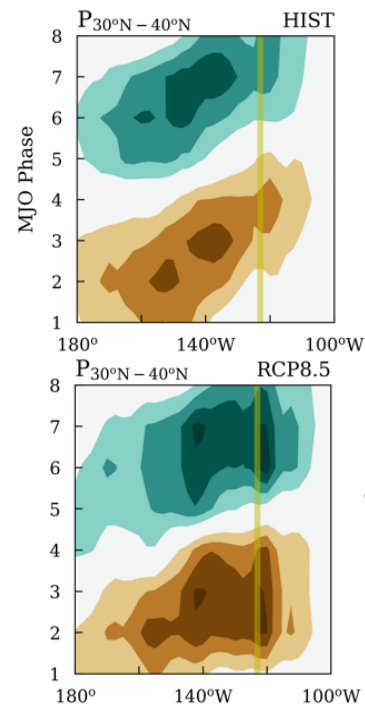
HIST



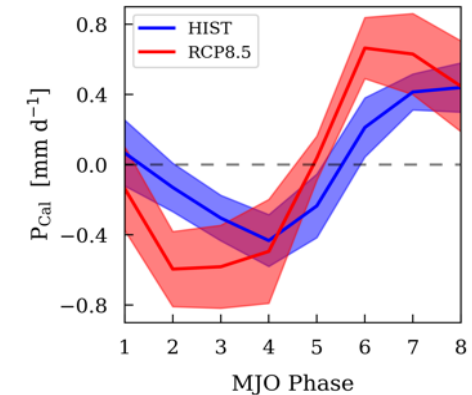
RCP8.5



MJO-phase-composited
 $30^{\circ}\text{N}-40^{\circ}\text{N}$ Precip



MJO-phase-composited
California Precip

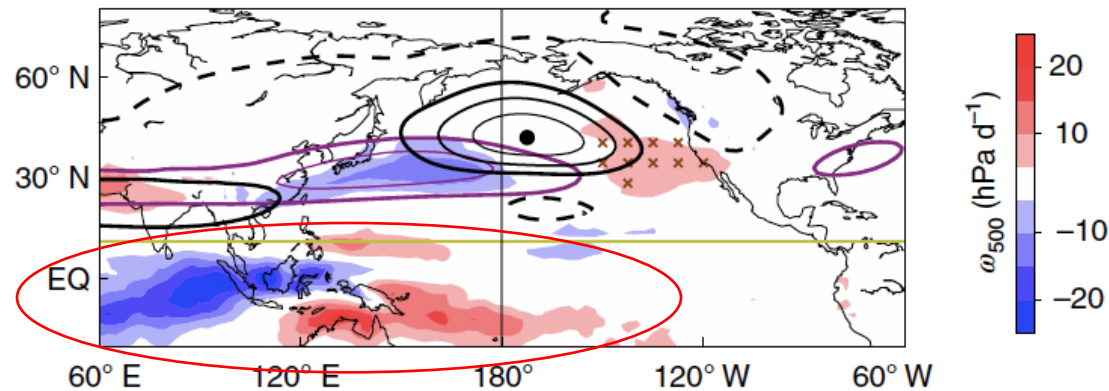


Causes of the eastward-extended MJO teleconnection?

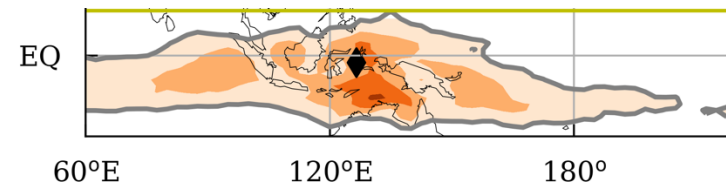
Phase 3, HIST

PNA-like pattern anchored on the exit of the subtropical jet

Z_{250} (black contours), ω_{500} (shading), Precip (cross)
 \bar{U}_{250} (black contours)



Reason 1: Eastward extension of the MJO itself

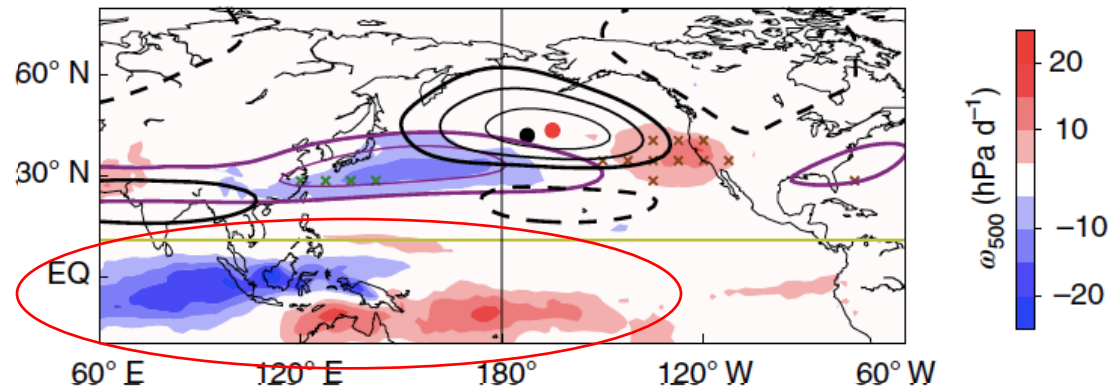


Causes of the eastward-extended MJO teleconnection?

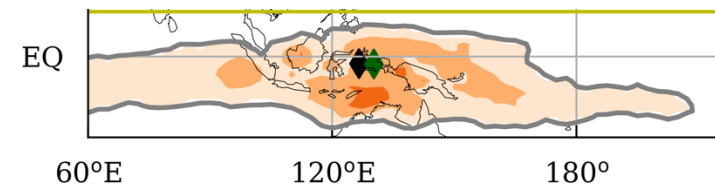
Phase 3, RCP8.5

PNA-like pattern anchored on the exit of the subtropical jet

Z_{250} (black contours), ω_{500} (shading), Precip (cross)
 \bar{U}_{250} (black contours)



Reason 1: Eastward extension of the MJO itself

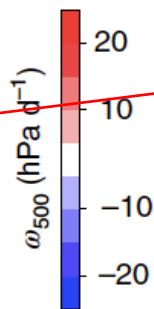
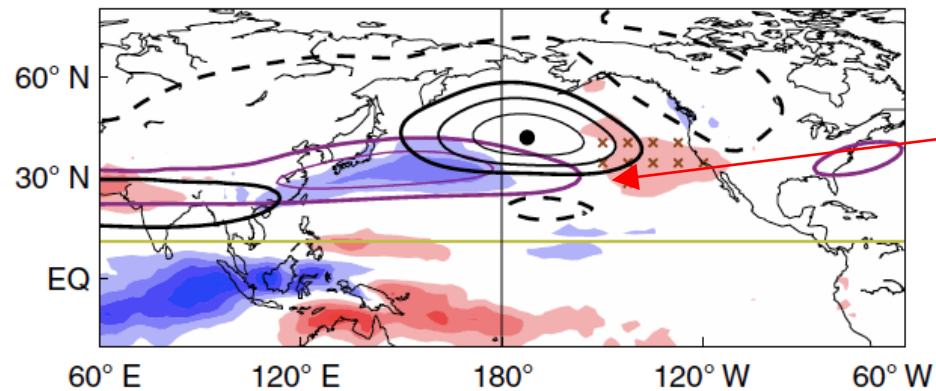


Causes of the eastward-extended MJO teleconnection?

Phase 3, HIST

PNA-like pattern anchored on the exit of the subtropical jet

Z_{250} (black contours), ω_{500} (shading), Precip (cross)
 \bar{U}_{250} (black contours)



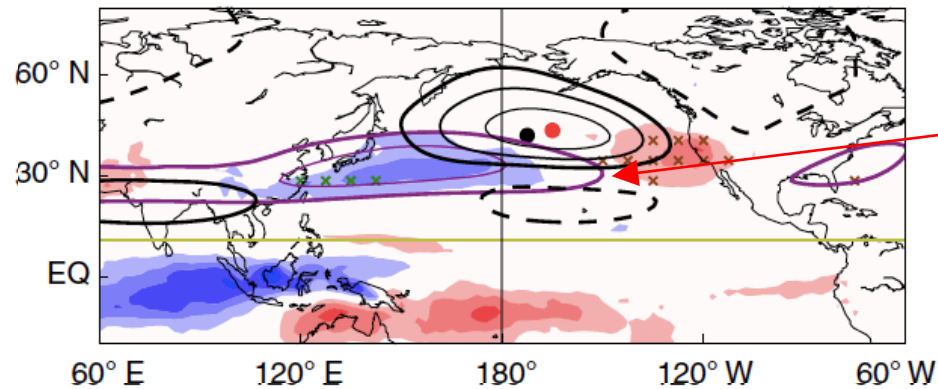
Reason 2: Eastward shift of the jet exit

Causes of the eastward-extended MJO teleconnection?

Phase 3, RCP8.5

PNA-like pattern anchored on the exit of the subtropical jet

Z_{250} (black contours), ω_{500} (shading), Precip (cross)
 \bar{U}_{250} (black contours)

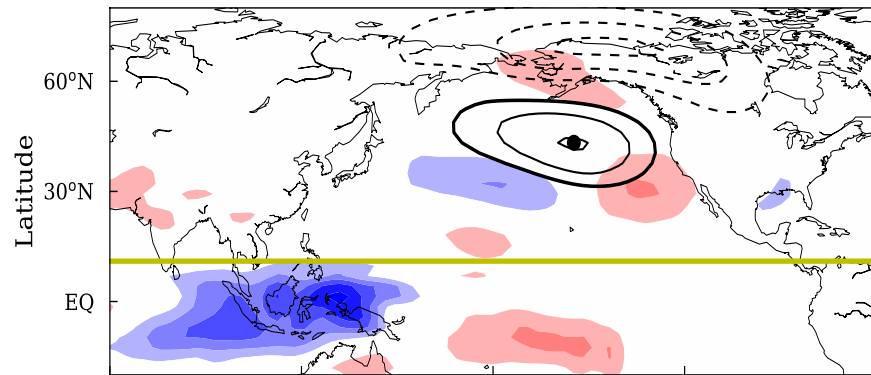


Reason 2: Eastward shift of the jet exit

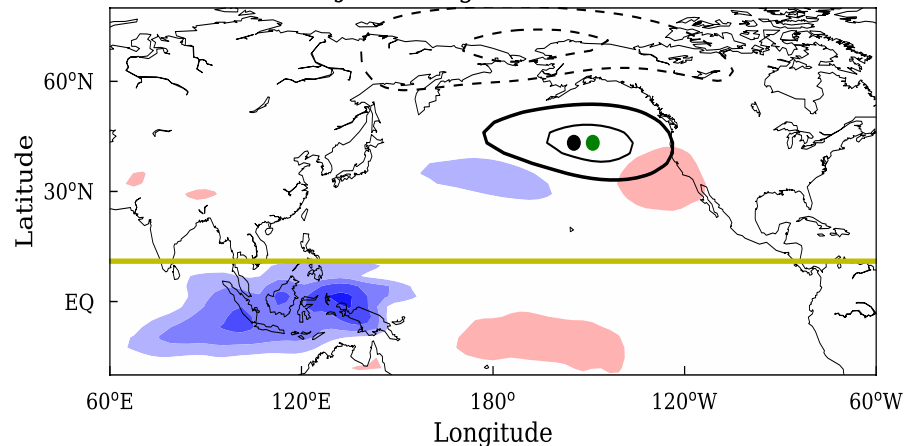
Linear Baroclinic Model experiments

Linear response to an eastward-propagating MJO heating
with prescribed large-scale mean state

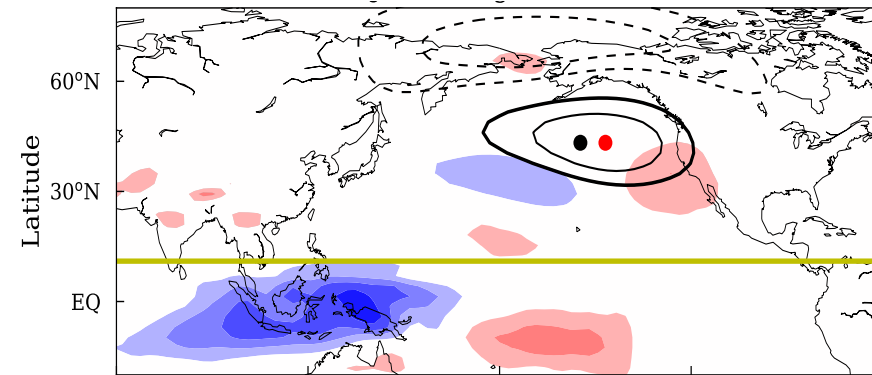
HIST Mean state and MJO heating



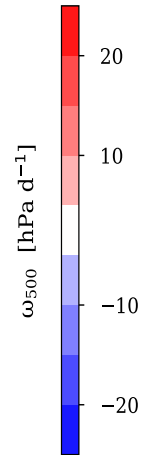
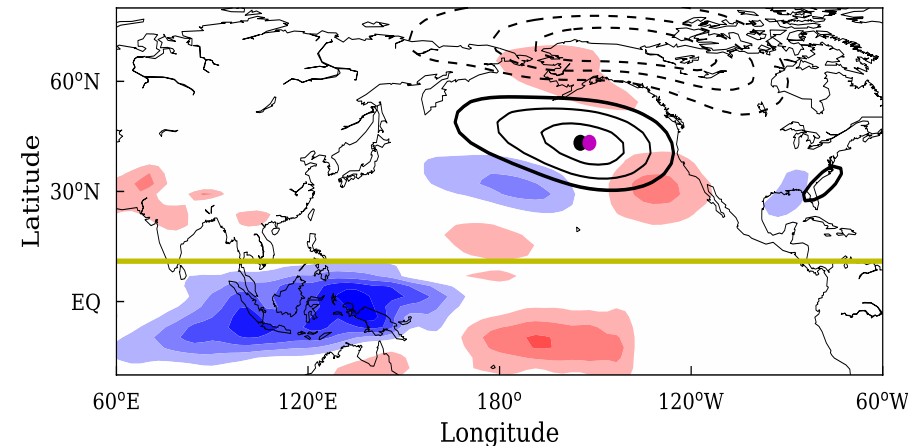
Mean state change only:
Eastward-shifted jet exit and increased static stability
(shift 6° and weaken)



RCP8.5 Mean state and MJO heating
(shift 8° and weaken slightly)

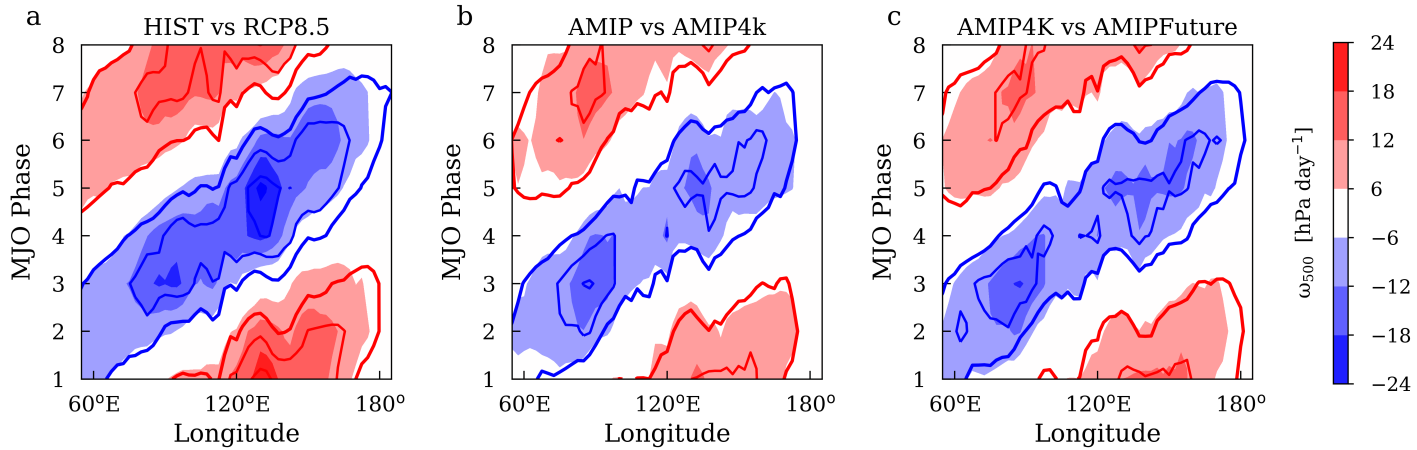


MJO heating change only:
Eastward-extended and amplified MJO heating
(shift 2° and intensify)



Equatorial warming pattern induces eastward extension of the MJO

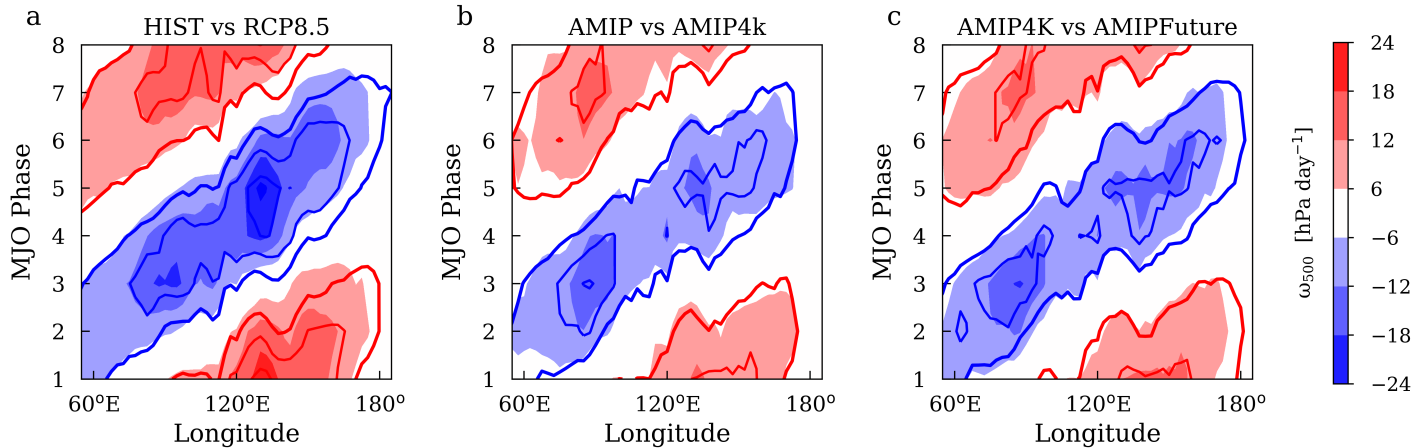
MJO-phase-composited 10°S - 10°N ω_{500}



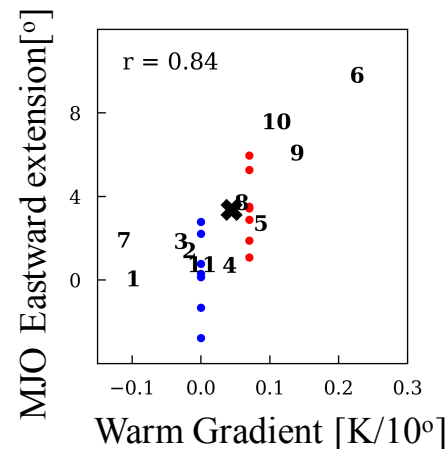
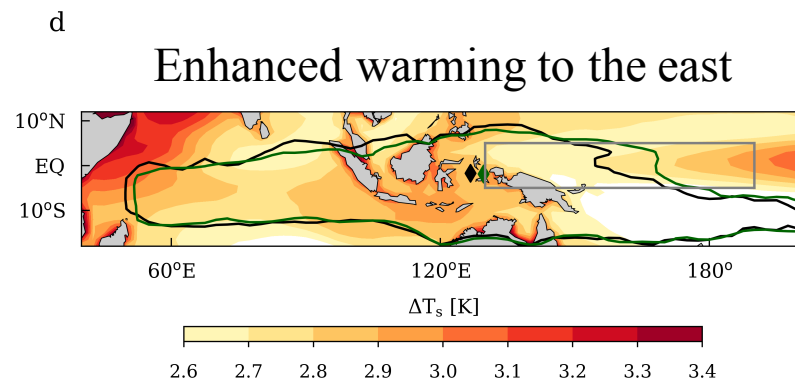
Eastward extension of MJO is only present in AMIPFuture with patterned warming.

Equatorial warming pattern induces eastward extension of the MJO

MJO-phase-composited $10^{\circ}\text{S}-10^{\circ}\text{N}$ ω_{500}



Eastward extension of MJO is only present in AMIPFuture with patterned warming.



The more Central Pacific is warmed compared to West Pacific, the more the MJO activity extends eastward.

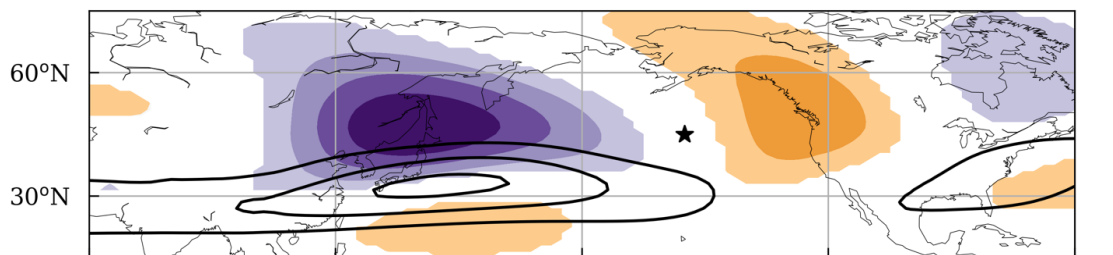
Eastward shifts of the boreal-winter stationary eddy pattern and the jet-exit

Eastward shift of the jet exit

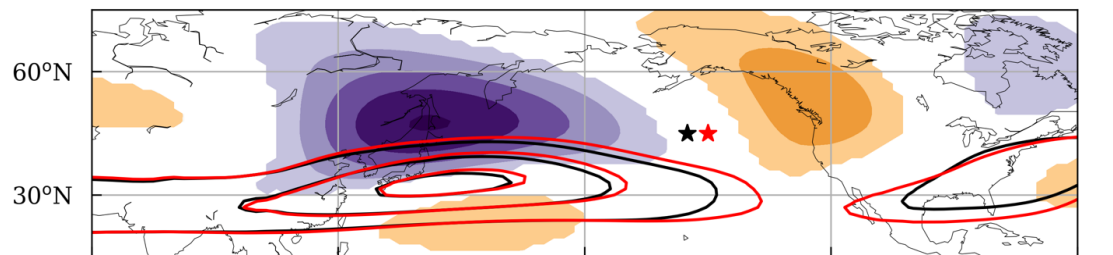


Eastward shift of the stationary eddy pattern

HIST



RCP8.5



60°E 120°E 180° 120°W 60°W

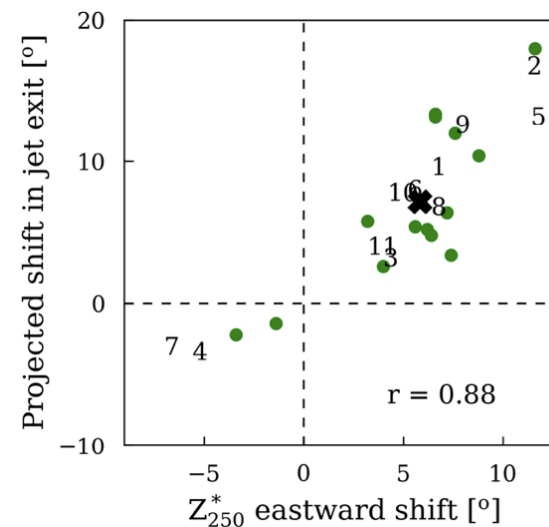
Z_{250}^* (shading) & U_{250} (contours)

Increased wavelength of stationary Rossby wave due to strengthened zonal wind (Simpson et al. 2016)

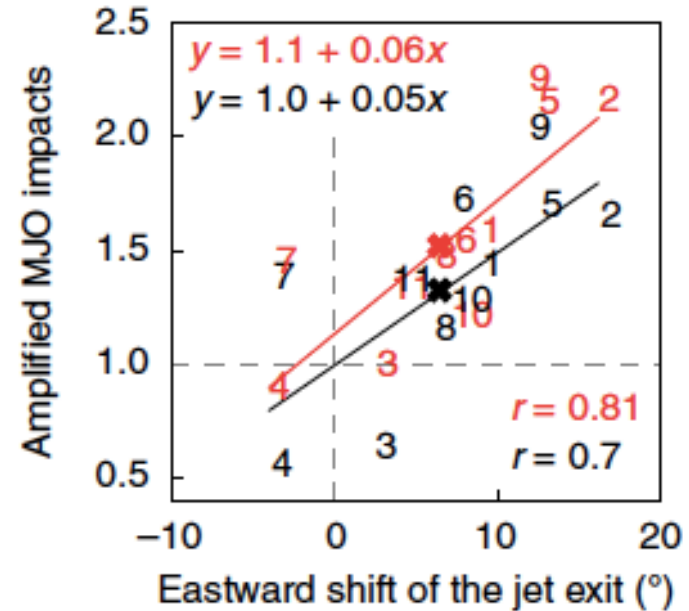
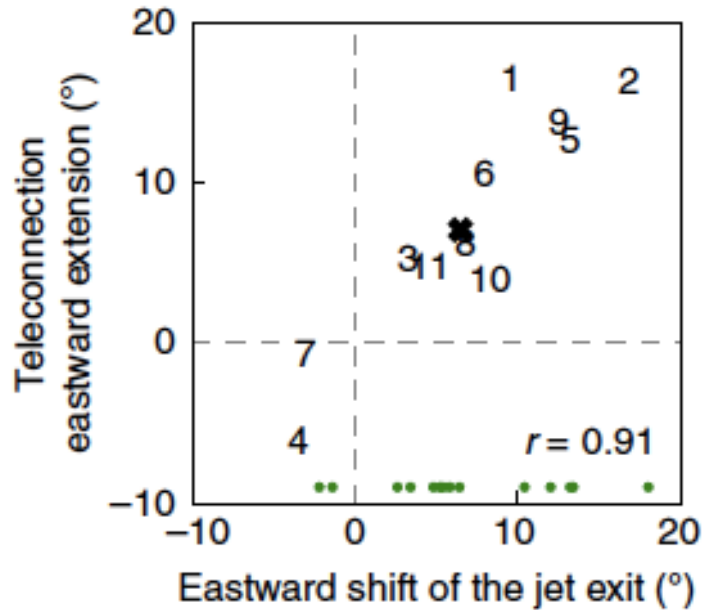
$$L \sim \sqrt{\frac{U}{\beta - U_{yy}}}$$

Numbers: selected models with good MJO

Green dots: unselected models



Amplified subseasonal variability of the California winter precipitation



ω_{500}
Precip

MME predicts a 32% (54%) increase in the MJO-induced ω_{500} (Precip) variability by 2100 under RCP8.5

1-degree eastward shift of the jet exit \rightarrow a \sim 5% (6%) increase in the MJO-induced ω_{500} (Precip) variability.

Summary

- MJO teleconnection pattern in the boreal-winter Pacific extends eastward under future warming, leading to amplified MJO impacts downstream in the PNA region.
- The eastward-extended teleconnection is primarily due to an eastward shift in the exit region of the subtropical jet, to which the teleconnection pattern is anchored, and additionally contributed from the eastward extension of the MJO itself.

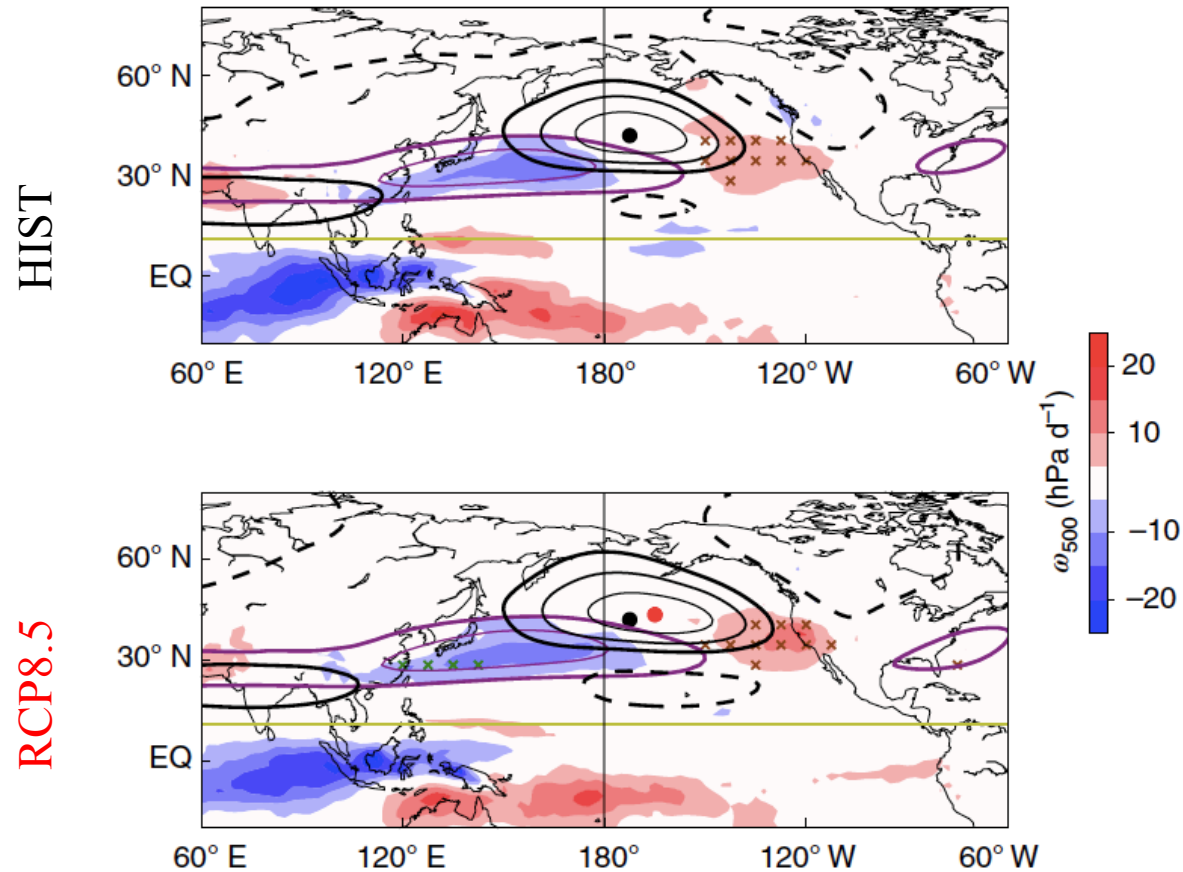
Implications

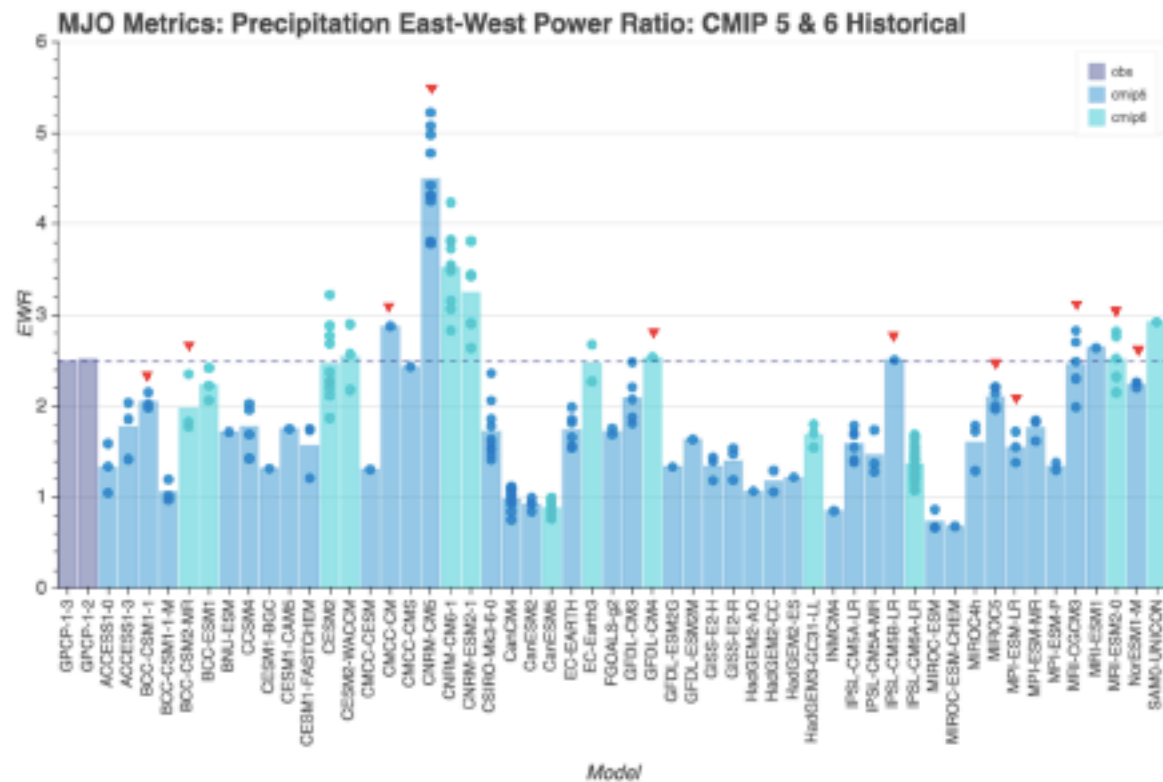
- Tropical-PNA teleconnection is projected to extend eastward in both MJO and ENSO cases, leading to amplified subseasonal and interannual variability in California. This poses acute challenges on regional resource management and extreme weather preparation.
- The eastward-extended PNA teleconnection implies increased predictability beyond week 2 over winter North America.

MJO teleconnection pattern extends eastward under future warming

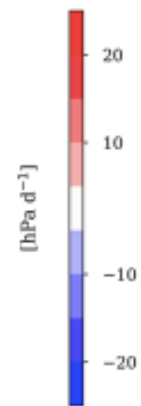
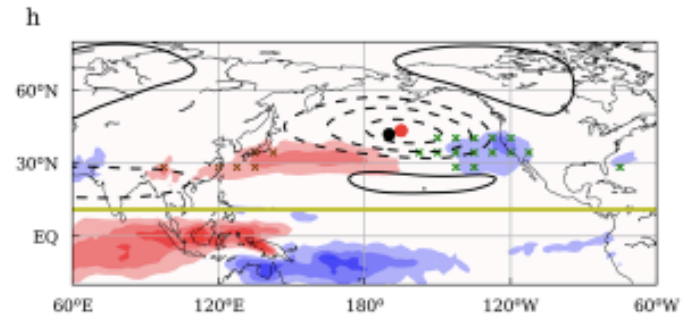
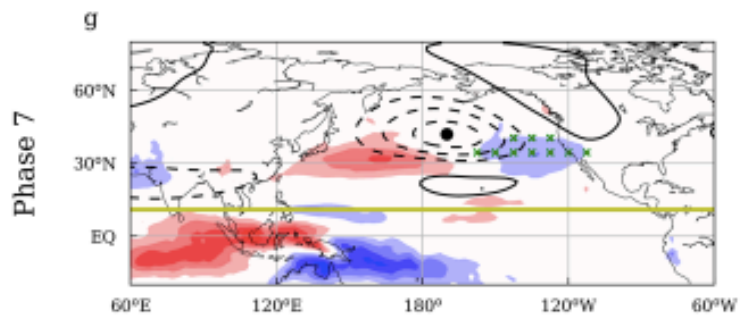
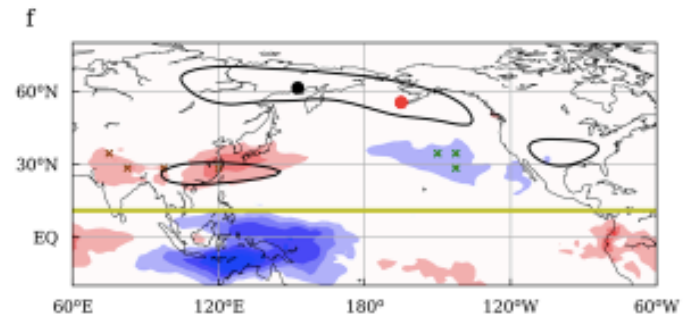
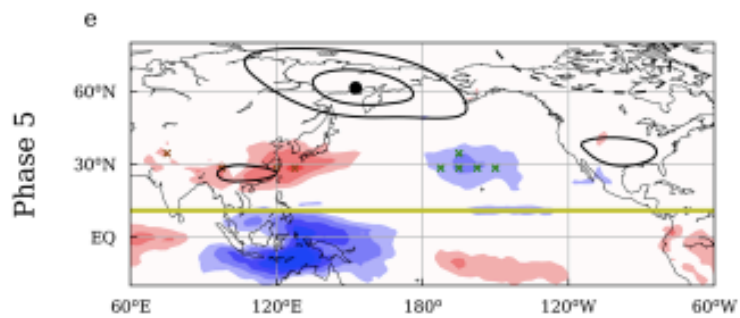
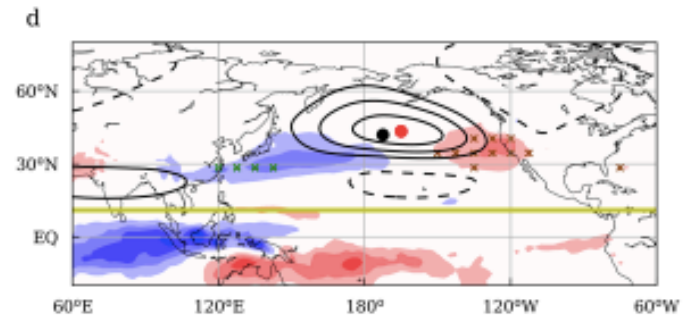
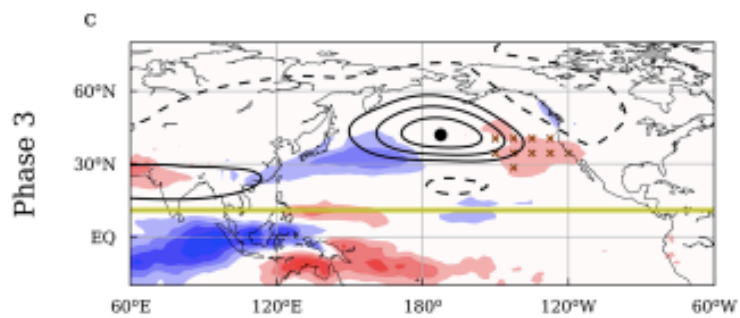
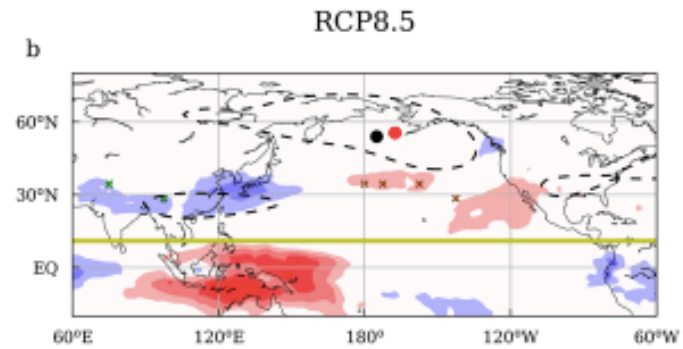
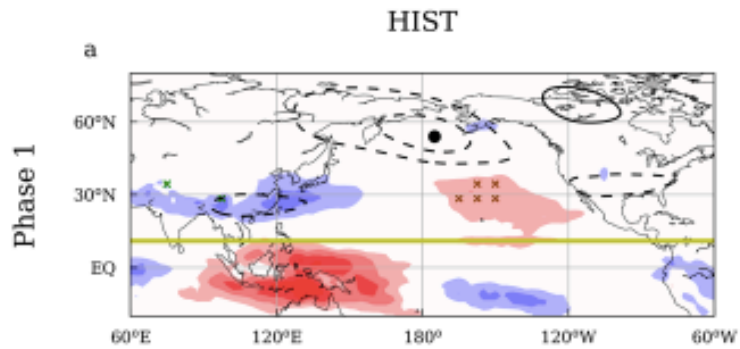
Phase 3 Composite

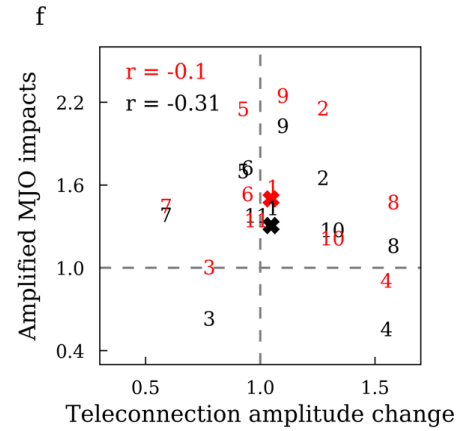
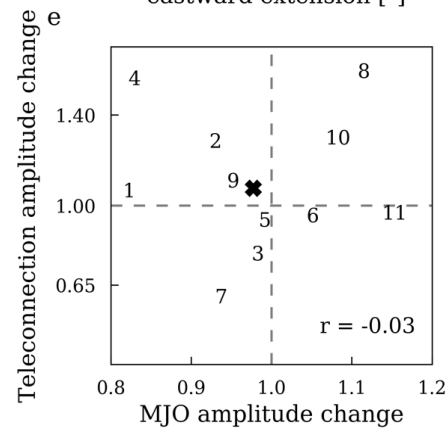
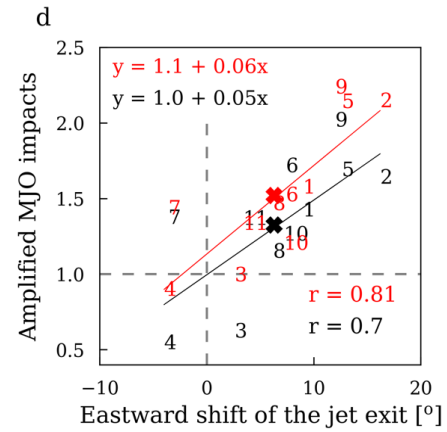
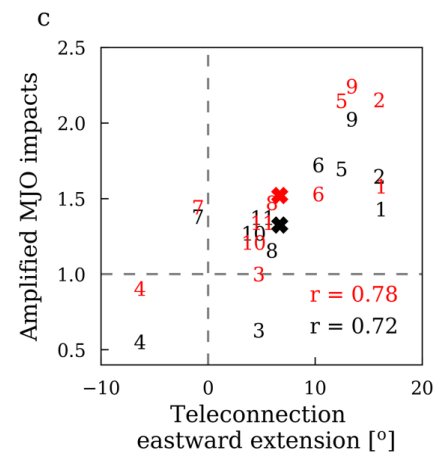
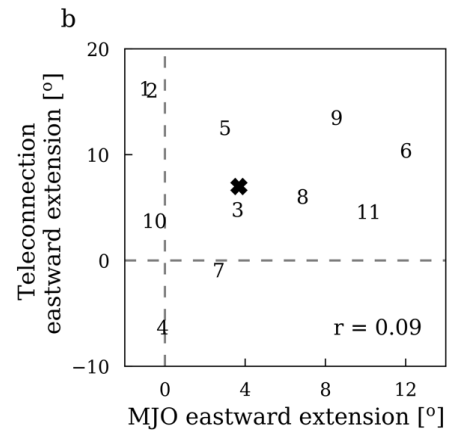
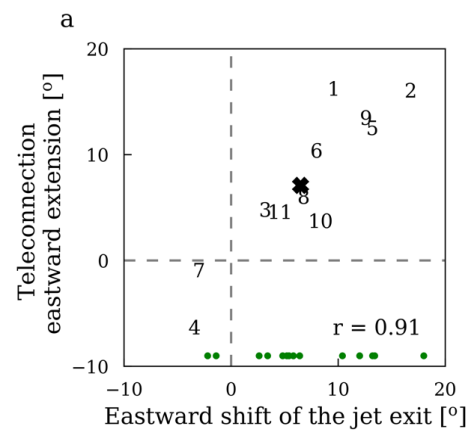
PNA-like pattern anchored on the exit of the subtropical jet
 Z_{250} (contours), ω_{500} (shading), Precip (cross)





Supplementary Figure 1: Precipitation East-West Power Ratio for models in CMIP5 and CMIP6. It is computed by the Program for Climate Model Diagnosis & Intercomparison (PCMDI) and available online at https://pcmdi.llnl.gov/pmp-preliminary-results/mjo_metrics/mjo_ewr_cmip5and6_overlap_runs_average_standalone.html. The 11 selected models are denoted by red triangles. The CESM2 and CNRM-CM6 also simulate reasonable East-West Power Ratio but both of them at this time lack daily outputs of required variables in the future projection.





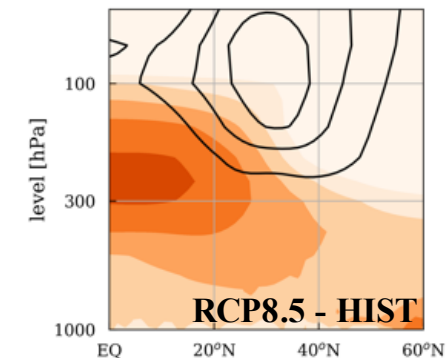
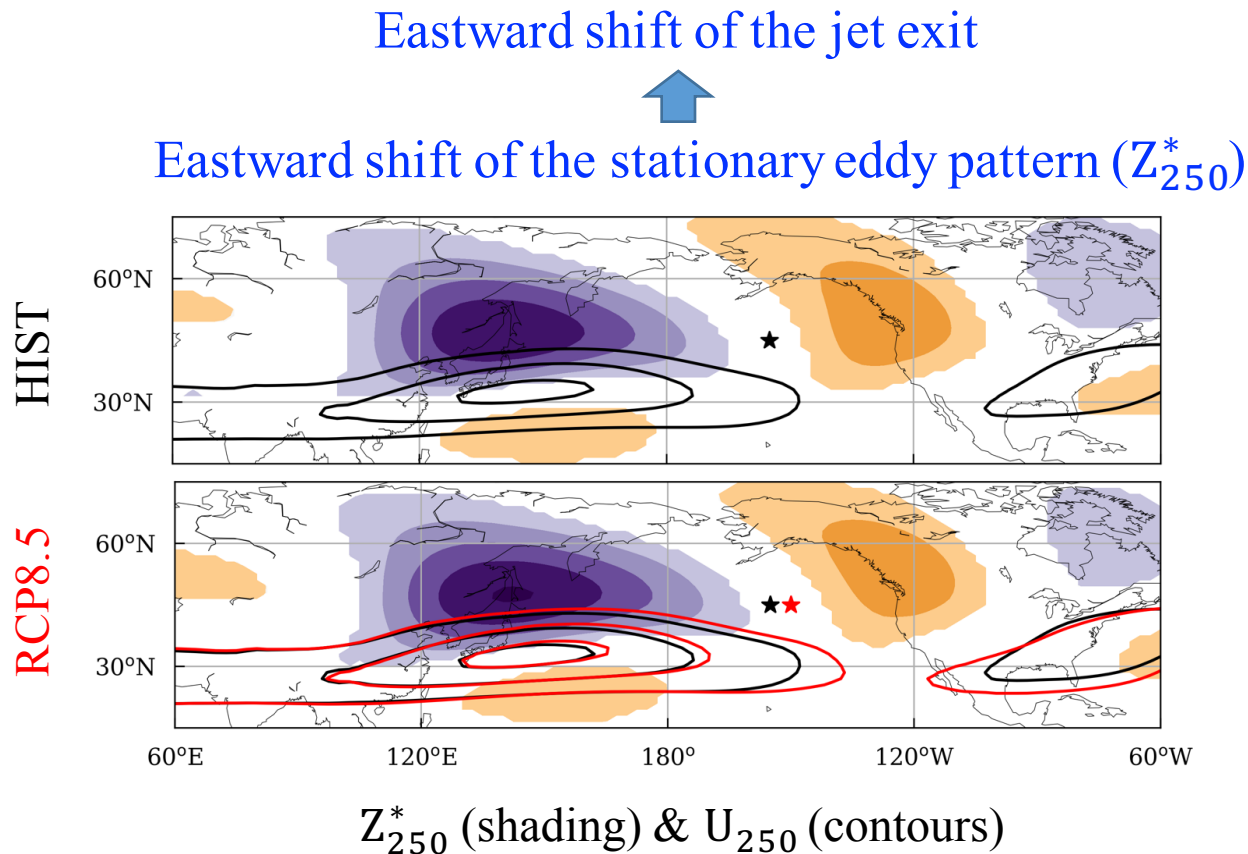
Eastward shifts of the stationary eddy pattern and thus the jet-exit shift

(Simpson et al. 2016)

Increased wavelength of stationary Rossby wave due to strengthened zonal wind

$$L \sim \sqrt{\frac{U}{\beta - U_{yy}}}$$

Under enhanced tropical upper-tropospheric warming



ΔT (shading) & ΔU (contours)